Scaling of genuine multiparticle entanglement close to a quantum phase transition

Martin Hofmann,[1] Andreas Osterloh,[2] and Otfried Gühne[1]

[1]*Naturwissenschaftlich-Technische Fakultät, Universität Siegen, Walter-Flex-Straße 3, 57068 Siegen, Germany*

[2]*Fakultät für Physik, Campus Duisburg, Universität Duisburg-Essen, Lotharstraße 1, 47048 Duisburg, Germany*

We investigate the scaling and spatial distribution of genuine multiparticle entanglement in three- and four-spin reduced states of the one-dimensional XY model at the quantum phase transition. We observe a logarithmic divergence, show that genuine three- and four-particle entanglement obeys finite-size scaling of the XY model and demonstrate that the genuine three-particle entanglement has a finite spatial range.

I. INTRODUCTION

In recent years it has turned out that quantum correlations play an important role in several branches of physics. One of these branches is the field of quantum optics and, more specifically, quantum information processing, where quantum correlations are often a useful resource for tasks such as quantum-enhanced precision measurements or quantum key distribution. Another branch is the field of condensed matter physics: Here, the study of entanglement in ground and thermal states of spin models has shed some light on the nature of quantum phase transitions [1–6], and at the same time has provided new insights into the simulation of spin models [7].

Most of the existing studies of entanglement in spin models, however, have restricted their attention to bipartite entanglement (for exemptions, see [5,8–11]): either, the entanglement in the reduced state of two particles of a multiparticle system was studied [1,2], or the entanglement between one block of particles and the remainder of the system [3]. In the latter case, the entanglement can often be related to the surface of the block, and these so-called area laws are an active research topic in mathematical physics [3,12] (for a review, see [13]). The restriction to two-party entanglement is due to the fact that the theory of entanglement for multiparticle systems is still not fully developed, and many open problems exist. Therefore, in the existing works on multiparticle entanglement in spin models [9–11] only bounds on the entanglement are given. In a complementary approach Batle *et al.* [14] investigated nonlocality in spin chains using Mermin inequalities. The presence of nonlocality, however, does not imply the presence of genuine multiparticle entanglement.

In this paper we study the scaling and spatial distribution of genuine multiparticle entanglement at a quantum phase transition in one-dimensional spin models. Our results are enabled by recent progress in the theory of multiparticle entanglement [15,16] in combination with an explicit determination of reduced k-particle states in the transverse XY model [17]. We consider a computable measure for genuine multiparticle entanglement for the reduced three- and four-particle states and demonstrate that its derivative diverges at the critical point. For both cases we show that the entanglement obeys finite-size scaling, which can be used to compute the critical exponent for the infinite system from finite-size data.

II. THE MODEL

We consider the one-dimensional XY model with transverse magnetic field on L particles and periodic boundary conditions [17]. The Hamiltonian of this model is given by

$$H = -\sum_{i=1}^{L} \frac{\lambda}{4}[(1+\gamma)\sigma_x^{(i)}\sigma_x^{(i+1)} + (1-\gamma)\sigma_y^{(i)}\sigma_y^{(i+1)}] + \frac{1}{2}\sigma_z^{(i)},$$

(1)

where the coupling constant $\lambda \geqslant 0$ tunes the strength of the nearest-neighbor coupling with respect to the external magnetic field. The parameter γ sets the anisotropy of the system and connects the Ising model ($\gamma = 1$) with the isotropic XY model ($\gamma = 0$). In the thermodynamic limit and for $0 < \gamma \leqslant 1$ the ground state of the model undergoes a quantum phase transition at the critical point $\lambda_c = 1$. For $\lambda = 0$ there is a unique ground state, where all spins are aligned in the direction of the magnetic field and there is no magnetization in the XY plane. For $\lambda \to \infty$ the ground state is twofold degenerate and hence is an equal mixture of these two states. At the quantum phase transition the systems ground state changes from being nondegenerate to degenerate, accompanied by an abrupt change of the magnetization in the x direction, which is zero for $\lambda < 1$ and finite for $\lambda \geqslant 1$. We use the XY model as a paradigm for our approach since it allows one to study a phase transition with analytical rigor [17]. In the following, we focus on the transverse Ising model ($\gamma = 1$), but our approach can be straightforwardly extended to the XY model.

III. GENUINE MULTIPARTICLE NEGATIVITY

Our tool to study genuine multiparticle entanglement in the reduced marginals of the ground state of the spin model is the genuine multiparticle negativity [15]. This mixed state entanglement monotone vanishes on all biseparable states and a nonzero value is a sufficient criterion for genuine multiparticle entanglement to be present. Let us sketch its main idea and give the related definitions for three parties, Alice (A), Bob (B), and Charlie (C); the generalization to more parties is straightforward.

First, recall that a three-particle state is fully separable and contains no entanglement, if it can be written as a statistical mixture of product states, that is, $\varrho^{\text{fulsep}} = \sum_k p_k |\psi_A^k\rangle\langle\psi_A^k| \otimes |\phi_B^k\rangle\langle\phi_B^k| \otimes |\phi_C^k\rangle\langle\phi_C^k|$. If the state is not fully separable, then it contains some entanglement, but it might be still separable

with respect to one of the splittings $A|BC$, $B|AC$, or $C|AB$. In this case it can be written as statistical mixture of states on the first system and joint states on the last two systems, for example, $\varrho_{A|BC}^{\text{sep}} = \sum_k p_k |\psi_A^k\rangle\langle\psi_A^k| \otimes |\phi_{BC}^k\rangle\langle\phi_{BC}^k|$. In this case, the state is called biseparable and not all three particles are entangled. Therefore, a state is called genuine multiparticle entangled [18] if it is not a mixture of biseparable states, that is, it can *not* be written as

$$\varrho^{\text{bisep}} = p_A \varrho_{A|BC}^{\text{sep}} + p_B \varrho_{B|AC}^{\text{sep}} + p_C \varrho_{C|AC}^{\text{sep}}. \tag{2}$$

Clearly, for genuine multiparticle entangled states all particles are entangled and therefore this is the most interesting form of multiparticle entanglement [19].

In order to study genuine multiparticle entanglement, it was proposed in Ref. [15] to consider so-called PPT (positive partial transpose) mixtures. These are of the form

$$\varrho^{\text{PPTmix}} = p_A \varrho_{A|BC}^{\text{PPT}} + p_B \varrho_{B|AC}^{\text{PPT}} + p_C \varrho_{C|AC}^{\text{PPT}}, \tag{3}$$

where $\varrho_{A|BC}^{\text{PPT}}$ is a state for which the partial transpose with respect to the partition $A|BC$ has no negative eigenvalues [20]. Since separable states are also PPT [21], the set of PPT mixtures is a superset of the biseparable states and hence all states which are not PPT mixtures are genuine multiparticle entangled. The advantage of the approach of Ref. [15] is that the question whether a state is a PPT mixture or not can be decided directly; moreover, although PPT mixtures are only an approximation, the resulting entanglement criteria are the strongest criteria known. In fact, for many families of states (e.g., permutationally invariant three-qubit states), they are even necessary and sufficient for genuine multiparticle entanglement [22].

The genuine multiparticle negativity N_ϱ is a measure to distinguish between states that are PPT mixtures and such that are not. It vanishes, if a decomposition into a PPT mixture exists and is nonzero elsewhere. Moreover, it was proven to be an entanglement monotone, since it cannot increase under local operations and classical communication [15]. At this point, we mention that it can be computed directly for a given density matrix via semidefinite programming; the precise formulation is given in Appendix Sec. 1.

IV. ENTANGLEMENT IN REDUCED THREE-QUBIT STATES

Let us start with the three-particle marginals of the ground state of the Ising model. Consider the particles i, j, and k in the systems ground state. For the Ising model we can always set i to be zero, since the XY Hamiltonian is translationally invariant and has periodic boundary conditions. The spatial arrangement of the particles is then completely described by $(\alpha,\beta) = (j - i, k - j)$, where (α,β) and (β,α) lead to the same reduced states due to mirror symmetry and hence one can choose $\alpha \leqslant \beta$ without loss of generality.

As a first task, we determined explicitly the reduced three-qubit states using the methods of Ref. [17]; detailed expressions are given in the Appendices Secs. 5–7. Evaluating the genuine multiparticle negativity for different spatial constellations in the thermodynamic limit $L \to \infty$ we find that for $(1,1)$ and $(1,2)$ the reduced marginals of the ground state are genuine multiparticle entangled in the vicinity of $\lambda = 1$
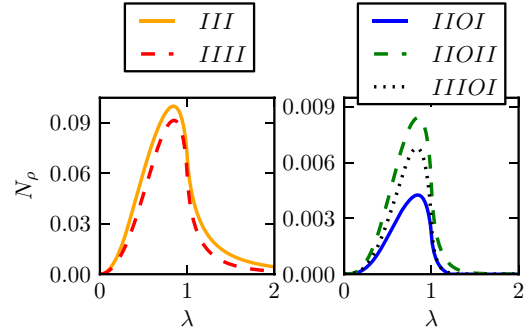

FIG. 1. (Color online) The genuine negativity N_ρ (for $L \to \infty$) as a function of λ for three- and four-particle reduced states in different spatial arrangements. On the left the values for three (III) or four ($IIII$) consecutive particles are shown. On the right-hand side, spatial arrangements for three and four particles which contain a single vacancy (denoted by 0) are shown. Here, $II0I$ denotes a three-particle reduced state in the qubits $\{i, i + 1, i + 3\}$ and $II0II$ denotes a four-particle reduced state in the qubits $\{i, i + 1, i + 3, i + 4\}$, etc. (see text for further details).

(see Fig. 1) and no entanglement is found if one separates the particles further. As the criterion of PPT mixtures is in general only a sufficient criterion for entanglement, the question arises whether for the separated configurations the reduced states are indeed biseparable. Concerning this point, it it first worth mentioning that so far no example of a genuinely entangled three-qubit state which cannot be detected by the PPT mixture approach is known. In our case, we can show even explicitly, using the algorithm for proving separability from Ref. [16], that the states are separable if the qubits are separated further (see Appendix Sec. 2). Using these results we also conclude that the genuine three-particle entanglement in the ground state stays short ranged and falls off to zero. It answers a discussion recently raised in Ref. [9]: In this reference, lower bounds on the entanglement were computed and no entanglement in the configuration $(1,2)$ was found, so it remained open, whether this or other configurations were separable. This makes us confident that the genuine multiparticle negativity is a well-suited tool for our analysis.

V. FINITE-SIZE SCALING

The observed divergence indicates that the system undergoes a phase transition. We study it in more detail using the finite-size scaling analysis [23,24]. This analysis is based on the idea that close to the phase transition at λ_c the behavior of a diverging quantity $P^{(L)}(\lambda)$ for finite system sizes L is governed by the system size L and a rescaled variable L/ξ only, with ξ being the correlation length. In the case of a logarithmic singularity of $P^{(L)}(\lambda)$, the finite-size scaling ansatz asserts the existence of a function Q, such that for finite L and λ close to the critical value [24]

$$P^{(L)}(\lambda) - P^{(L)}(\lambda_0) \sim Q(L^{1/\nu}|\lambda - \lambda_c|) - Q(L^{1/\nu}|\lambda_0 - \lambda_c|). \tag{4}$$

Here ν is the critical exponent, which governs the divergence of the correlation length $\xi \sim |\lambda - \lambda_c|^{-\nu}$ close to the critical
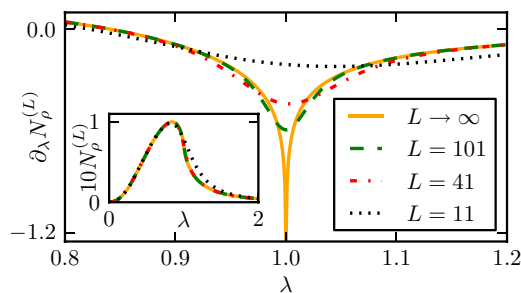
FIG. 2. (Color online) In the thermodynamic limit the first derivative of the genuine negativity with respect to λ diverges at the quantum phase transition. For finite chain lengths $L = 11$ (dotted line), $L = 41$ (dashed dotted line), and $L = 101$ (dashed line) there is a minimum in the vicinity of the critical point $\lambda_c = 1$, which gets smaller for increasing L, diverging in the limit $L \to \infty$. The subplot shows the genuine negativity depending on λ for different chain lengths in a larger region around the critical point.

value as $L \to \infty$. For the ansatz to consistently recover

$$P^{(\infty)}(\lambda) \sim C_\infty \ln |\lambda - \lambda_c| \qquad \text{as} \quad \lambda \to \lambda_c \qquad (5)$$

in the thermodynamic limit, one sets $Q(z) \sim C_\infty \ln z$ for $z \to \infty$. Provided that $Q(z) = \text{const}$ as $z \to 0$

$$P^{(L)}[\lambda_c(L)] \sim -\frac{C_\infty}{\nu} \ln L + \text{const} \qquad (6)$$

the minimum in $P^{(L)}$ at the pseudocritical value diverges with the system size L, such that Eqs. (5) and (6) allow one to determine the critical exponent ν.

For the two-particle entanglement, it was already shown that finite-size scaling holds [1]. In the multiparticle case, the quantity of interest is the derivative of the multiparticle negativity. So we vary the particle number L, keeping the arrangement $(1,1)$ fixed, and study the three-particle genuine negativity $N_\rho^{(L)}$ together with its first derivative $\partial_\lambda N_\rho^{(L)}$ (see Fig. 2). One observes a logarithmic divergence of $\partial_\lambda N_\rho^{(\infty)}$ at $\lambda_c = 1$. This is where the quantum phase transition occurs. There is distinct minimum in $\partial\lambda N_\rho^{(L)}$ for finite system sizes L at $\lambda_c(L)$ which we take to be the pseudocritical value. We find that it approaches the critical value like $\lambda_c(L) - \lambda_c \sim L^{-\kappa}$ with a shift exponent $\kappa = 2.19$ [25].

Fitting the expected behavior to our data as done in Fig. 3, one recovers the critical exponent, which is known to be $\nu = 1$, since

$$\partial_\lambda N_\varrho^{(\infty)} = 0.170 \ln(|\lambda - \lambda_c|) + 0.267, \qquad (7)$$

$$\partial_\lambda N_\varrho^{(L)}[\lambda_c(L)] = -0.170 \ln L + 0.191, \qquad (8)$$

for sufficiently big L. We performed the same analysis on the genuine negativity for the arrangements $(1,2)$ and observed similar qualitative results. Note that the numerical accuracy of the fitting procedure is higher than the displayed accuracy; a more detailed discussion is given in Appendix Sec. 3.

The finite-size scaling analysis shows that the behavior of the genuine multiparticle entanglement close to the critical point is governed by the quantum phase transition. A divergent behavior alone may be expected from the results of Ref. [4], as the reduced two-particle density matrix of the ground state
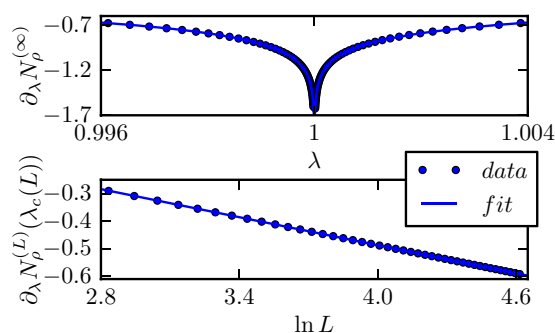

FIG. 3. (Color online) Evaluation of the minima for different chain lengths and the divergence in the thermodynamic limit (circles) of the first derivative of the genuine negativity for three consecutive particles shows the behavior expected (lines) from the scaling ansatz for a logarithmic divergence. In the upper graph the divergence of the genuine negativity is plotted with respect to the coupling parameter λ close to the critical point $\lambda_c = 1$. The lower plot shows that minimum at the pseudocritical value $\lambda_c(L)$ scales linear with the logarithm of the chain length L.

itself is nonanalytical [26]. Indeed many investigations of lower bounds on genuine multiparticle entanglement show this behavior [9–11]. On the flip side none of these investigations allowed one to draw conclusions with respect to the critical attributes of the system. The finite-size scaling, however, shows that multiparticle entanglement faithfully represents important properties of the spin system at the critical point; moreover, it may be used for the extrapolation of critical exponents from finite-size numerical simulations.

VI. ENTANGLEMENT IN REDUCED FOUR-QUBIT STATES

As in the previous part, the density matrices of four particles $i < j < k < l$ depend on the spacing between the particles $\alpha = j - i, \beta = k - j$, and $\delta = l - k$ and the coupling parameter λ only. Here we may choose $\alpha \leqslant \delta$ due to symmetry.

We find that there are three spatial arrangements with nonzero genuine negativity. These are the tightest packed constellations $(1,1,1)$ and the constellations $(1,1,2)$ and $(1,2,1)$. Further separated constellations yield a zero genuine negativity. We observe that with increasing separation the four-particle genuine negativity decreases with increasing separation. This is similar to the three-particle case. On the other hand, the genuine negativity for the four-particle arrangements with one intermediate particle $(1,1,2)$ and $(1,2,1)$ is much larger than the comparable three-particle case $(1,2)$ (see Fig. 1). Taking into account that for the tightest conformations $(1,1)$ [respectively, $(1,1,1)$] the values are quite close to each other, the four-particle genuine multiparticle entanglement seems to be more uniformly distributed throughout the system.

In addition, we tested the four-concurrence, defined on pure states as $C_4(\psi) := \langle \psi^* | \sigma_y \otimes \sigma_y \otimes \sigma_y \otimes \sigma_y | \psi \rangle$ and analytically extendable to mixed states [27] on this model, and it qualitatively behaves roughly the same way, except for single distribution patterns. Since C_4 is nonzero only for products of two-particle Bell states and the GHZ_4-type of states, this observation suggests two possible scenarios: either the state is a mixture of Bell products, not seen by N_ρ plus states from

the null cone (for example W_4 states), or it really contains GHZ$_4$-type entanglement. Further studies in this direction are needed in order to clarify this issue.

The finite-size scaling analysis for four consecutive particles $(1,1,1)$ yields results similar to the three-particle case but is more subject to numerical errors due to error propagation. For separations $(1,2,1)$ and $(1,1,2)$ the first derivative of the genuine negativity shows a qualitatively similar scaling behavior as in the case where all four particles are in succession. A full discussion is given in Appendix Sec. 4.

VII. DISCUSSION

Using the Ising model in a transverse magnetic field, we investigated the connection between genuine multiparticle entanglement and quantum phase transitions. We identified the configurations of three and four particles where entanglement is present and showed that the derivative of the genuine multiparticle negativity diverges logarithmically at the critical points. We further confirmed that this quantity obeys a finite-size scaling behavior close to the quantum phase transition.

Besides its fundamental interest, there are several consequences and applications of our work. First, as our method allows the direct study of multiparticle entanglement, it can be used to complete existing indirect results on multiparticle entanglement. To give an example, in Ref. [5] the existence of multiparticle entanglement in the one-dimensional XYZ model was concluded indirectly from monogamy relations, and possible connections to phase transitions were found. Our approach allows one to verify these results in a direct manner. Similarly, in Ref. [8] the two-partite negativities for different splittings of three particles in the XY model were studied; our methods can now decide whether these bipartite quantities are connected to genuine multiparticle entanglement. Further, in Ref. [10] certain three-particle reduced states could neither be detected as genuine multiparticle entangled nor shown to be biseparable. We expect that an application of our method would solve this issue. Second, our results demonstrate the usefulness of the genuine multiparticle negativity to study many-body systems. This makes it applicable to further systems, such as dynamical phase transitions [28], quenching dynamics, or the study of symmetry breaking [10].

APPENDIX

1. Mathematical definition of the multiparticle negativity

Mathematically, the genuine multiparticle negativity is defined as optimization over the set of fully decomposable witnesses W; these witnesses have to fulfill certain constraints [15]. In total, the optimization problem reads for three

particles:

$$N_\varrho = -\min_W \, \mathrm{tr}(W\varrho)$$

such that for all $m \in \{A,B,C\}$

$$W = P_m + Q_m^{T_m}, \quad 0 \leqslant P_m, \quad Q_m \leqslant \mathbb{1}. \quad \text{(A1)}$$

As all these conditions are linear or semidefinite constraints, this problem can be solved with the method of semidefinite programming, and the optimality of the solution can be verified. A simple, ready-to-use implementation can be found on line [29].

2. Separability of three and four qubits

In our work we supplement the entanglement monotone with a separability algorithm [16]. The idea of the algorithm is to decompose ϱ into two biseparable parts

$$\varrho = (1-p)\varrho_a + p\varrho_b, \quad \text{(A2)}$$

such that ϱ_b is a statistical mixture of pure separable states and ϱ_a is within the ball of separable states around the completely mixed state [30]. The algorithm is performed iteratively such that the purity of ϱ_a is decreased with each successful step until ϱ_a lies within the set of separable states proving the separability of ϱ.

Given an input state ϱ, we define $\varrho = \varrho_0$ and iterate the following procedure:

(1) Find a pure biseparable state $|\psi_k\rangle$ which has large overlap with $\sqrt{\varrho_k}$. It will add to the part ϱ_b in the decomposition (A2). We take random states and choose the one with the largest overlap.

(2) Choose $0 \leqslant \varepsilon_k \leqslant 1$, such that $\varrho_{k+1} = \frac{1}{1-\varepsilon_k}(\varrho_k - \varepsilon_k|\psi_k\rangle\langle\psi_k|)$ is positive semidefinite. This ensures that ϱ is indeed a convex combination of all $|\psi_k\rangle\langle\psi_k|$ and ϱ_{k+1}. Note that the algorithm seems to be more reliable, if ε_k is significantly smaller than the smallest eigenvalue of ϱ.

(3) Check whether $\mathrm{tr}(\varrho_{k+1}^2) < \frac{1}{7}$ and thus if ϱ_{k+1} is separable for some bipartition [30].

(4) If this is the case, than the algorithm finishes and ϱ is separable, else continue until some maximal iteration number is reached.

In practice the algorithm performs good on all full rank states; if, however, the state has eigenvalues close to zero it fails to detect separable states as such. This is due to the fact that ρ_0 is initially close to the border of separable states and hence during iterations ρ_k might leave the set of separable states. In such a case the algorithm cannot bring back ρ_k into the separable ball around the completely mixed state and the algorithm does not detect the state as separable.

Using local filtering one can significantly improve the algorithms ability to detect separable states with small eigenvalues. The idea is to apply invertible local matrices to the state $\varrho \mapsto \mathcal{F}_1 \otimes \mathcal{F}_2 \otimes \mathcal{F}_3 \varrho \mathcal{F}_1^\dagger \otimes \mathcal{F}_2^\dagger \otimes \mathcal{F}_3^\dagger$, such that the smallest eigenvalue of the normalized new state increases. This new state is then more likely to be detected by the algorithm if it is separable. Since both states are connected by invertible local operations the separability of one state implies the separability of the other. Using this modification we can, on the one hand, decrease the number of iterations the algorithm needs to show the separability of a separable state. On the other hand, we are
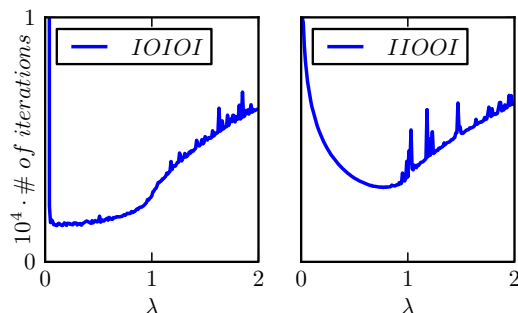
FIG. 4. (Color online) The number of iteration steps of the separability algorithm needed to show separability is shown with respect to the coupling parameter λ for the particle constellations (1,3) (right) as well as for (2,2) (left). For most cases the algorithm converges in less than 10^4 steps proving the separability of the respective states. For $\lambda = 0$ we know that the reduced state is pure and separable. For $\lambda \to 0$ the underlying state has small eigenvalues. Here the algorithm does not prove separability, even though these states are separable as well.
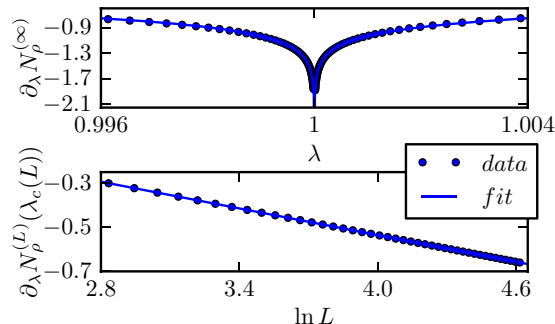

FIG. 5. (Color online) Evaluation of the minima for different chain lengths and the divergence in the thermodynamic limit (circles) of the first derivative of the genuine negativity for four consecutive particles shows the scaling behavior expected (lines) from the scaling ansatz for a logarithmic divergence. On top the genuine negativity is plotted with respect to λ diverging logarithmically at the critical point. The mid plot confirms the ansatz made with respect to the L dependence of position of the minima, and the lower plot shows the predicted behavior of the value of the minima with respect to different chain lengths.

able to detect separable states, which are not detected by the unmodified algorithm.

Our investigations of the three-particle reduced states in the thermodynamic limit for the particle separation other than (1,1) and (1,2) result in a vanishing genuine multiparticle negativity. Applying the algorithm to states of the constellations (1,3) and (2,2) confirms that these reduced three-particle marginals are separable (see Fig. 4).

3. Four successive particles scaling analysis

The scaling analysis in the case of four closely packed particles (1,1,1) is along the line of the three-particle case. It yields similar results as in the three-particle case (see Fig. 5):

$$\partial_\lambda N_\varrho^{(\infty)} = 0.20 \ln(|\lambda - \lambda_c|) + 0.36, \tag{A3}$$

$$\partial_\lambda L_\varrho^{(L)}[\lambda_c(L)] = -0.20 \ln L + 0.27. \tag{A4}$$

The negative quotient of the logarithmic prefactors again give way to the expected critical exponent of the diverging correlation length $\nu = 1$. Due to numerical precision, however, the determination of the position and value of the minima was more subtle than in the three-particle case. Specifically, a faithful determination of the position of the minima was impossible for $L > 33$ due to numerical inaccuracies, which we

discuss in the next section in this Appendix. The determination of the absolute value of the minima, however, suffered less from these problems and made it possible to confirm the expected scaling.

4. Discussion of numerical precision

For the derivation of our results we make use of the genuine negativity [15], which is implemented via semidefinite programming. It provides an upper bound of how far the numerical value obtained is from the global optimum. One can take this bound as a conservative error for the genuine negativity. In our calculations the absolute error of the genuine negativity is of the order of 10^{-14}. This error is negligible, if one considers the genuine negativity itself. For the finite-size scaling analysis, however, this error has to be taken into account. Recall that in the scaling analysis one has to extract several minima of the first derivative of the genuine negativity. The first derivative is approximated with the central finite difference method,

$$f' \approx \frac{-f(x + 2h) + 8f(x + h) - 8f(x - h) + f(x - 2h)}{12h}, \tag{A5}$$

and the forward and backward finite differences close to the divergence,

$$f' \approx \frac{-25f(x) + 48f(x + h) - 36f(x + 2h) + 16f(x + 3h) - 3f(x + 4h)}{12h},$$

$$f' \approx \frac{+25f(x) - 48f(x - h) + 36f(x - 2h) - 16f(x - 3h) + 3f(x - 4h)}{12h}. \tag{A6}$$

We found $h = 10^{-7}$ to give us optimal results. The absolute error of the genuine negativity results in an absolute leading error in the first derivative. It is of the order of 10^{-7} and

hence the overall precision in estimating the position and absolute value of the minimum in the first derivative of the genuine negativity is limited. This directly influences how

well one can perform the finite-size scaling analysis. In the case of three (1,1) and four (1,1,1) consecutive particles one can find the position of these minima with sufficient high precision up to $L = 33$ particles and their values up to $L = 100$ particles, which is sufficient for the finite-size scaling analysis. For a larger number of particles, however, the errors of the positions and values of the minima caused growing errors in the coefficients of the fitting functions. This finally makes the extraction of the critical exponent ν impossible. Hence, we omitted a quantitative finite-size scaling analysis in these cases.

5. Diagonalizing the *XY* model

We give a brief review of the analytical diagonalization of

$$H = -\sum_{i=1}^{L} \frac{\lambda}{4}\left[(1+\gamma)\sigma_x^{(i)}\sigma_x^{(i+1)} + (1-\gamma)\sigma_y^{(i)}\sigma_y^{(i+1)}\right] + \frac{1}{2}\sigma_z^{(i)}.$$

$$(A7)$$

The strategy is as follows [17].

(1) First, we apply the so-called Jordan-Wigner transformation, which maps the model onto a fermionic Fock space with creation and annihilation operators.

(2) Second, the transformed system decouples into a direct sum of four-dimensional Hilbert spaces by using discrete Fourier transformation.

(3) Finally, these subspaces can be diagonalized, giving access to the ground state, the energy spectrum, and expectation values of finite products of one-site Pauli operators.

First, apply the Jordan-Wigner transformation, which transforms the spin operators S_j^α, $j = 1, \ldots, L$, $\alpha = x,y,z$ into fermionic creators $c_j^\dagger$ and annihilators c_j. It is composed of two intermediate transformations

$$a_j^\dagger = \sigma_x^j + i\sigma_y^j \quad \text{and} \quad a_j = \sigma_x^j - i\sigma_y^j, \quad (A8)$$

where $a_j^\dagger$ and a_j are hard-core bosonic creation and annihilation operators. The fermionic operators are then obtained by

$$c_j = \exp\left\{\pi i \sum_{k=1}^{j-1} a_k^\dagger a_k\right\} a_j, \quad c_j^\dagger = a_j^\dagger \exp\left\{-\pi i \sum_{k=1}^{j-1} a_k^\dagger a_k\right\}.$$

$$(A9)$$

The new operators obey the fermionic anticommutation algebra

$$\{c_i^\dagger, c_j\} = \delta_{ij} \quad \text{and} \quad \{c_i, c_j\} = \{c_i^\dagger, c_j^\dagger\} = 0. \quad (A10)$$

Applying the Jordan-Wigner transformation to the Hamiltonian (A7) yields

$$H = \frac{L}{2} + \frac{\lambda}{2}[(c_L^\dagger c_1 + \gamma c_L^\dagger c_1) + \text{H.c.}]$$

$$\times \left(\exp\left\{i\pi \sum_{j=1}^{L} c_j^\dagger c_j\right\} + 1\right)$$

$$- \frac{\lambda}{2}\sum_{i=1}^{L}(c_i^\dagger c_{i+1} + \gamma c_i^\dagger c_{i+1}^\dagger) + \text{H.c.} + c_i^\dagger c_i, \quad (A11)$$

where H.c. denotes the Hermitian conjugate of the parenthesized expression in front. For L large the second term can be neglected. For odd L the second term vanishes. Thus by restriction to an odd number of particles, one can continue the diagonalization procedure with the Hamiltonian

$$H = \frac{L}{2} - \sum_{i=1}^{L} \frac{\lambda}{2}(c_i^\dagger c_{i+1} + \gamma c_i^\dagger c_{i+1}^\dagger) + \text{H.c.} + c_i^\dagger c_i. \quad (A12)$$

Next, one performs a Fourier transform to decouple the Hamiltonian into a direct product of Hilbert spaces preserving the fermionic anticommutation relations. Let $\phi_p = 2\pi p/L$; then the operators c_i are given in the new operators b_p as

$$c_j = \frac{1}{\sqrt{L}} \sum_{p=-L/2}^{L/2} \exp(-ij\phi_p)b_p, \quad (A13)$$

where the summation runs over all possible momenta. Applying the Fourier transform (A13) to the Hamiltonian (A12) results in

$$H = \frac{L}{2} - (\lambda+1)b_0^\dagger b_0 - \sum_{p=1}^{L/2}(\lambda\cos\phi_p + 1)(b_p^\dagger b_p + b_{-p}^\dagger b_{-p})$$

$$- i\gamma\lambda\sin\phi_p(b_p^\dagger b_{-p}^\dagger + b_p b_{-p}). \quad (A14)$$

The Hilbert space decomposes into noninteracting subspaces. The space of zero momentum is two dimensional and already diagonal, whereas the other subspaces are four dimensional and nondiagonal.

In order to diagonalize the remaining subspaces in the Hamiltonian (A14) let $\alpha_p = (\lambda\cos\phi_p + 1)$, $\beta_p = \lambda\gamma\sin\phi_p$, and use then the canonically transformed operators

$$\eta_k = \tilde{\alpha}_k b_{-k} - i\tilde{\beta}_k b_k^\dagger, \quad (A15)$$

with

$$\tilde{\alpha}_k = \frac{\Lambda_k - \alpha_k}{\sqrt{2\left(\Lambda_k^2 - \Lambda_k\alpha_k\right)}},$$

$$\tilde{\beta}_k = \frac{\beta_k}{\sqrt{2\left(\Lambda_k^2 - \Lambda_k\alpha_k\right)}}, \quad \text{and} \quad (A16)$$

$$\Lambda_k = \sqrt{\alpha_k^2 + \beta_k^2}.$$

In the new creation and annihilation operators $\eta_k^\dagger$ and η_k our Hamiltonian reads

$$H = \sum_{k=-L/2}^{L/2} \Lambda_k \eta_k^\dagger \eta_k - \frac{1}{2}\sum_k \Lambda_k. \quad (A17)$$

Clearly, the ground state of the system is given by the Fock vacuum in the fermionic basis. Although the vacuum state is separable in the fermionic basis this does not have to hold for the computational basis, since the Jordan-Wigner transformation is a global unitary transformation. To draw conclusions about the entanglement properties of the ground

state one has to study the ground state in the computational basis.

6. Expectation values of Pauli operators

In order to calculate the three-particle [8] (respectively, four-particle) reduced density matrices of the ground state $|0\rangle$ of our system one has to trace out all particles but three (respectively, four). Alternatively one can choose a local operator basis on each system, which is not to be traced out and calculate the one-point up to four-point correlators to recover the reduced density matrix. For the reduced states on the three particles i, j, and k and the four particles i, j, k, and l this would yield

$$\varrho_{ijk} = \frac{1}{8} \sum_{m,n,o} \langle \sigma_i^m \sigma_j^n \sigma_k^o \rangle_{|0\rangle} \sigma_i^m \sigma_j^n \sigma_k^o \quad \text{and} \quad \text{(A18)}$$

$$\varrho_{ijkl} = \frac{1}{16} \sum_{m,n,o,p} \langle \sigma_i^m \sigma_j^n \sigma_k^o \sigma_l^p \rangle_{|0\rangle} \sigma_i^m \sigma_j^n \sigma_k^o \sigma_l^p, \quad \text{(A19)}$$

where each of the summations m, n, o, and p run over $\{x, y, z, 0\}$. In order to calculate the expectation values $\langle \sigma_{i_1}^{\alpha_1} \cdots \sigma_{i_k}^{\alpha_k} \rangle_{|0\rangle}$ one needs to express the Pauli operators in terms of the fermionic operators $\eta_k^\dagger$ and η_k. It is

$$\sigma_l^x = (c_l + c_l^\dagger) \prod_{i=1}^{l-1} (c_i^\dagger + c_i)(c_i^\dagger - c_i),$$

$$\sigma_l^z = -(c_l^\dagger + c_l)(c_l^\dagger - c_l), \quad \text{(A20)}$$

$$\sigma_l^y = -i(c_l^\dagger - c_l) \prod_{i=1}^{l-1} (c_i^\dagger + c_i)(c_i^\dagger - c_i),$$

and thus the Pauli operators are products of

$$A_l = c_l + c_l^\dagger = \frac{1}{\sqrt{L}} \sum_q (\eta_{-q}^\dagger + \eta_q)(\alpha_q + i\beta_q)e^{i\phi_q l}, \quad \text{(A21)}$$

$$B_l = c_l - c_l^\dagger = \frac{1}{\sqrt{L}} \sum_q (-\eta_{-q}^\dagger + \eta_q)(\alpha_q - i\beta_q)e^{i\phi_q l}, \quad \text{(A22)}$$

which are linear in the creation and annihilation operators $\eta_i^\dagger$ (respectively, η_i). The expectation values of arbitrary tensor

products of

$$\sigma_l^x = A_l \prod_{i=1}^{l-1} A_i B_i, \quad \sigma_l^z = -A_i B_i, \quad \sigma_l^y = -i B_l \prod_{i=1}^{l-1} A_i B_i \quad \text{(A23)}$$

are then monomials in the fermionic creation and annihilation operators. These can be evaluated using the Wick theorem, which states the equality

$$\langle \mathcal{O}_1 \cdots \mathcal{O}_n \rangle_{|0\rangle}$$
$$= \langle \mathcal{O}_1 \mathcal{O}_2 \rangle_{|0\rangle} \langle \mathcal{O}_3 \cdots \mathcal{O}_n \rangle_{|0\rangle} - \langle \mathcal{O}_1 \mathcal{O}_3 \rangle_{|0\rangle}$$
$$\times \langle \mathcal{O}_2 \mathcal{O}_4 \cdots \mathcal{O}_n \rangle_{|0\rangle} + \langle \mathcal{O}_1 \mathcal{O}_4 \rangle_{|0\rangle} \cdots, \quad \text{(A24)}$$

where $\mathcal{O}_i$ can be any operator A_j or B_k. Successive application of the theorem reduces the expectation values in (A18) and its four-particle counterpart (A19) to products of the two-point expectation values $\langle A_l A_k \rangle_{|0\rangle}$, $\langle A_l B_k \rangle_{|0\rangle}$, and $\langle B_l B_k \rangle_{|0\rangle}$. Using Eqs. (A21) and (A22) and setting $r = k - l$ one can calculate these to be

$$\langle A_l A_k \rangle_{|0\rangle} = \delta_{lk}, \quad \text{(A25)}$$

$$\langle A_l B_k \rangle_{|0\rangle} = \frac{2}{\pi} \int_0^\pi d\phi [\cos\phi r(1 + \lambda\cos\phi)$$
$$- \gamma\lambda\sin\phi\sin\phi r]\frac{1}{\Lambda_\phi}, \quad \text{(A26)}$$

$$\langle B_l B_k \rangle_{|0\rangle} = -\delta_{lk} \quad \text{(A27)}$$

in the thermodynamic limit. For finite L Eq. (A26) is given by

$$\langle A_l B_k \rangle_{|0\rangle} = \frac{1}{L} \sum_q \frac{1}{\Lambda_q} [\cos r\phi_q(1 + \lambda\cos\phi_q)$$
$$- \gamma\lambda\sin\phi_q\sin r\phi_q]. \quad \text{(A28)}$$

To evaluate $\langle \sigma_i^m \sigma_j^n \sigma_k^o \rangle_{|0\rangle}$ and $\langle \sigma_i^m \sigma_j^n \sigma_k^o \sigma_l^p \rangle_{|0\rangle}$ we express the Pauli operators in terms of A_j or B_k. Then proceed with the general scheme by Ref. [31]. Reorder the operators with respect to the fermionic commutation relations, such that all A_l are in front of the B_l and both are in ascending order. After this step the expressions look like

$$\pm \langle A_{i_1} \cdots A_{i_k} B_{j_1} \cdots B_{j_k} \rangle_{|0\rangle}. \quad \text{(A29)}$$

Applying the Wick theorem iteratively one obtains the following Pfaffian:

$$\pm pf \begin{bmatrix} 0 & \langle A_{i_1} A_{i_2} \rangle_{|0\rangle} & \cdots & \langle A_{i_1} A_{i_k} \rangle_{|0\rangle} & \langle A_{i_1} B_{j_1} \rangle_{|0\rangle} & \cdots & \langle A_{i_1} B_{j_k} \rangle_{|0\rangle} \\ -\langle A_{i_1} A_{i_2} \rangle_{|0\rangle} & 0 & & \langle A_{i_2} A_{i_k} \rangle_{|0\rangle} & \langle A_{i_2} B_{j_1} \rangle_{|0\rangle} & & \langle A_{i_2} B_{j_k} \rangle_{|0\rangle} \\ & & \vdots & \vdots & & \vdots \\ & & \ddots & \langle A_{i_{k-1}} A_{i_k} \rangle_{|0\rangle} & \langle A_{i_{k-1}} B_{j_1} \rangle_{|0\rangle} & & \langle A_{i_{k-1}} B_{j_k} \rangle_{|0\rangle} \\ & & & 0 & \langle A_{i_k} B_{j_1} \rangle_{|0\rangle} & \cdots & \langle A_{i_k} B_{j_k} \rangle_{|0\rangle} \\ & & & & 0 & \cdots & \langle B_{j_1} B_{j_k} \rangle_{|0\rangle} \\ & & & & & \vdots \\ & & & & & \ddots & \langle B_{j_{k-1}} B_{j_k} \rangle_{|0\rangle} \\ & & & & & & 0 \end{bmatrix}. \quad \text{(A30)}$$

Note that the upper left and the lower right $k \times k$ block of this Pfaffian are zero, since we have $i_1 < i_2 < \cdots < i_k$ and $j_1 < j_2 < \cdots < j_k$ together with (A25) and (A27). Such a Pfaffian can be expressed as

$$pf \begin{bmatrix} 0 & M \\ -M^T & 0 \end{bmatrix} = (-1)^{k(k-1)/2} \det M \qquad (A31)$$

and therefore we have

$$\langle A_{i_1} \cdots A_{i_k} B_{j_1} \cdots B_{j_k} \rangle_{|0\rangle}$$

$$= (-1)^{k(k-1)/2} \begin{vmatrix} G_{j_1-i_1} & \cdots & G_{j_k-i_1} \\ \vdots & & \vdots \\ G_{j_1-i_k} & \cdots & G_{j_k-i_k} \end{vmatrix}, \qquad (A32)$$

where $G_{k-l} = \langle A_l B_k \rangle_{|0\rangle}$.

7. Expectation values of four-site operator basis

A list of all nonzero expectation values of the four-site Pauli operators $\langle \sigma_i^m \sigma_j^n \sigma_k^o \sigma_l^p \rangle_{|0\rangle}$ is presented here. The three-site expectation values are omitted, since they are already contained in those of four sites. Note that there are 80 nonvanishing expectation values out of 256. This is due to several symmetries the Hamiltonian possesses, and which carry over to its ground state. Namely, the Hamiltonian is translationally invariant and thus just the spacings $\alpha = j - i$, $\beta = k - j$, and $\delta = k - l$ between the local sites enter the final expectation values. Furthermore, it is invariant under global x flip $\sigma_i^x \to -\sigma_i^x$ for all i and under global y flip. Hence the only contribution to the four-site Pauli operators are those in which σ^x and σ^y appear an even number of times. The exact numerical value finally depends on $\langle A_l B_k \rangle_{|0\rangle} = G_{k-l}$ only. It is

$$\langle \mathbb{1}\mathbb{1}\mathbb{1}\mathbb{1} \rangle_{|0\rangle} = 1,$$
$$\langle \sigma_i^z \mathbb{1}\mathbb{1}\mathbb{1} \rangle_{|0\rangle} = -G_0, \qquad (A33)$$
$$\langle \sigma_i^z \sigma_j^z \mathbb{1}\mathbb{1} \rangle_{|0\rangle} = G_0^2 - G_\alpha G_{-\alpha}.$$

Similarly it is $\langle \mathbb{1}\sigma_j^z \mathbb{1}\mathbb{1} \rangle_{|0\rangle} = \langle \mathbb{1}\mathbb{1}\sigma_k^z \mathbb{1} \rangle_{|0\rangle} = \langle \mathbb{1}\mathbb{1}\mathbb{1}\sigma_l^z \rangle_{|0\rangle} = -G_0$. As for the tensor product of two σ^z operators $\langle \sigma_i^z \mathbb{1}\sigma_k^z \mathbb{1} \rangle_{|0\rangle} = G_0^2 - G_{\alpha+\beta} G_{-\alpha-\beta}$, $\langle \sigma_i^z \mathbb{1}\mathbb{1}\sigma_l^z \rangle_{|0\rangle} = G_0^2 - G_{\alpha+\beta+\delta} G_{-\alpha-\beta-\delta}$, $\langle \mathbb{1}\sigma_j^z \sigma_k^z \mathbb{1} \rangle_{|0\rangle} = G_0^2 - G_\beta G_{-\beta}$, $\langle \mathbb{1}\sigma_j^z \mathbb{1}\sigma_j^z \rangle_{|0\rangle} = G_0^2 - G_{\beta+\delta} G_{-\beta-\delta}$, and $\langle \mathbb{1}\mathbb{1}\sigma_k^z \sigma_l^z \rangle_{|0\rangle} = G_0^2 - G_\delta G_{-\delta}$.

$$\langle \sigma_i^z \sigma_j^z \sigma_k^z \mathbb{1} \rangle_{|0\rangle} = -\begin{vmatrix} G_0 & G_\alpha & G_{\alpha+\beta} \\ G_{-\alpha} & G_0 & G_\beta \\ G_{-\alpha-\beta} & G_{-\beta} & G_0 \end{vmatrix}. \qquad (A34)$$

To get the expectation values of the other possible permutations of the above operator one simply has to perform the following replacements (applied from left to right): $\langle \sigma_i^z \sigma_j^z \mathbb{1}\sigma_l^z \rangle_{|0\rangle} : \beta \to \beta + \delta$, $\langle \sigma_i^z \mathbb{1}\sigma_k^z \sigma_l^z \rangle_{|0\rangle} : \beta \to \delta \wedge \alpha \to \alpha + \beta$, and $\langle \mathbb{1}\sigma_j^z \sigma_k^z \sigma_l^z \rangle_{|0\rangle} : \beta \to \delta \wedge \alpha \to \beta$.

$$\langle \sigma_i^z \sigma_j^z \sigma_k^z \sigma_l^z \rangle_{|0\rangle} = \begin{vmatrix} G_0 & G_\alpha & G_{\alpha+\beta} & G_{\alpha+\beta+\delta} \\ G_{-\alpha} & G_0 & G_\beta & G_{\beta+\delta} \\ G_{-\alpha-\beta} & G_{-\beta} & G_0 & G_\delta \\ G_{-\alpha-\beta-\delta} & G_{-\beta-\delta} & G_{-\delta} & G_0 \end{vmatrix}, \qquad (A35)$$

$$\langle \sigma_i^x \sigma_j^x \mathbb{1}\mathbb{1} \rangle_{|0\rangle} = (-1)^\alpha \begin{vmatrix} G_{-1} & \cdots & G_{\alpha-2} \\ \vdots & & \vdots \\ G_{-\alpha} & \cdots & G_{-1} \end{vmatrix}, \qquad (A36)$$

$\langle \sigma_i^x \mathbb{1}\sigma_k^x \mathbb{1} \rangle_{|0\rangle} : \alpha \to \alpha + \beta$, $\langle \sigma_i^x \mathbb{1}\mathbb{1}\sigma_l^x \rangle_{|0\rangle} : \alpha \to \alpha + \beta + \delta$, $\langle \mathbb{1}\sigma_j^x \sigma_k^x \mathbb{1} \rangle_{|0\rangle} : \alpha \to \beta$, $\langle \mathbb{1}\sigma_j^x \mathbb{1}\sigma_l^x \rangle_{|0\rangle} : \alpha \to \beta + \delta$, and $\langle \mathbb{1}\mathbb{1}\sigma_k^x \sigma_l^x \rangle_{|0\rangle} : \alpha \to \delta$.

$$\langle \sigma_i^x \sigma_j^x \sigma_k^z \mathbb{1} \rangle_{|0\rangle} = (-1)^{\alpha+1} \begin{vmatrix} G_{-1} & \cdots & G_{\alpha-2} & G_{\alpha+\beta-1} \\ \vdots & & \vdots & \vdots \\ G_{-\alpha} & \cdots & G_{-1} & G_\beta \\ G_{-\alpha-\beta} & \cdots & G_{-\beta-1} & G_0 \end{vmatrix}, \qquad (A37)$$

$\langle \sigma_i^x \sigma_j^x \mathbb{1}\sigma_l^z \rangle_{|0\rangle} : \beta \to \beta + \delta$, $\langle \sigma_i^x \mathbb{1}\sigma_k^x \sigma_l^z \rangle_{|0\rangle} : \beta \to \delta \wedge \alpha \to \alpha + \beta$, and $\langle \mathbb{1}\sigma_j^x \sigma_k^x \sigma_l^z \rangle_{|0\rangle} : \beta \to \delta \wedge \alpha \to \beta$.

$$\langle \sigma_i^x \sigma_j^z \sigma_k^x \mathbb{1} \rangle_{|0\rangle} = (-1)^{\alpha+\beta} \begin{vmatrix} G_{-1} & \cdots & G_{\alpha-2} & G_\alpha & \cdots & G_{\alpha+\beta-2} \\ \vdots & & \vdots & \vdots & & \vdots \\ G_{-\alpha+1} & \cdots & G_0 & G_2 & \cdots & G_\beta \\ G_{-\alpha-1} & \cdots & G_{-2} & G_0 & \cdots & G_{\beta-2} \\ \vdots & & \vdots & \vdots & & \vdots \\ G_{-\alpha-\beta} & \cdots & G_{-\beta-1} & G_{-\beta+1} & \cdots & G_{-1} \end{vmatrix}, \qquad (A38)$$

$\langle \sigma_i^x \sigma_j^z \mathbb{1} \sigma_l^x \rangle_{|0\rangle} : \beta \to \beta + \delta$, $\langle \sigma_i^x \mathbb{1} \sigma_k^z \sigma_l^x \rangle_{|0\rangle} : \beta \to \delta \wedge \alpha \to \alpha + \beta$, and $\langle \mathbb{1} \sigma_j^x \sigma_k^z \sigma_l^x \rangle_{|0\rangle} : \beta \to \delta \wedge \alpha \to \beta$.

$$\langle \sigma_i^z \sigma_j^x \sigma_k^x \mathbb{1} \rangle_{|0\rangle} = (-1)^{\beta+1} \begin{vmatrix} G_0 & G_\alpha & \cdots & G_{\alpha+\beta-1} \\ G_{-\alpha-1} & G_{-1} & \cdots & G_{\beta-2} \\ \vdots & \vdots & & \vdots \\ G_{-\alpha-\beta} & G_{-\beta} & \cdots & G_{-1} \end{vmatrix}, \tag{A39}$$

$\langle \sigma_i^z \sigma_j^x \mathbb{1} \sigma_l^x \rangle_{|0\rangle} : \beta \to \beta + \delta$, $\langle \sigma_i^z \mathbb{1} \sigma_k^x \sigma_l^x \rangle_{|0\rangle} : \beta \to \delta \wedge \alpha \to \alpha + \beta$, and $\langle \mathbb{1} \sigma_j^z \sigma_k^x \sigma_l^x \rangle_{|0\rangle} : \beta \to \delta \wedge \alpha \to \beta$.

$$\langle \sigma_i^y \sigma_j^y \mathbb{1} \mathbb{1} \rangle_{|0\rangle} = (-1)^\alpha \begin{vmatrix} G_1 & \cdots & G_\alpha \\ \vdots & & \vdots \\ G_{-\alpha+2} & \cdots & G_1 \end{vmatrix}, \tag{A40}$$

$\langle \sigma_i^y \mathbb{1} \sigma_k^y \mathbb{1} \rangle_{|0\rangle} : \alpha \to \alpha + \beta$, $\langle \sigma_i^y \mathbb{1} \mathbb{1} \sigma_l^y \rangle_{|0\rangle} : \alpha \to \alpha + \beta + \delta$, $\langle \mathbb{1} \sigma_j^y \sigma_k^y \mathbb{1} \rangle_{|0\rangle} : \alpha \to \beta$, $\langle \mathbb{1} \sigma_j^y \mathbb{1} \sigma_l^y \rangle_{|0\rangle} : \alpha \to \beta + \delta$, and $\langle \mathbb{1} \mathbb{1} \sigma_k^y \sigma_l^y \rangle_{|0\rangle} : \alpha \to \delta$.

$$\langle \sigma_i^y \sigma_j^y \sigma_k^z \mathbb{1} \rangle_{|0\rangle} = (-1)^{\alpha+1} \begin{vmatrix} G_1 & \cdots & G_\alpha & G_{\alpha+\beta} \\ \vdots & & \vdots & \vdots \\ G_{-\alpha+2} & \cdots & G_1 & G_{\beta+1} \\ G_{-\alpha-\beta+1} & \cdots & G_{-\beta} & G_0 \end{vmatrix}, \tag{A41}$$

$\langle \sigma_i^y \sigma_j^y \mathbb{1} \sigma_l^z \rangle_{|0\rangle} : \beta \to \beta + \delta$, $\langle \sigma_i^y \mathbb{1} \sigma_k^y \sigma_l^z \rangle_{|0\rangle} : \beta \to \delta \wedge \alpha \to \alpha + \beta$, and $\langle \mathbb{1} \sigma_j^y \sigma_k^y \sigma_l^z \rangle_{|0\rangle} : \beta \to \delta \wedge \alpha \to \beta$.

$$\langle \sigma_i^y \sigma_j^z \sigma_k^y \mathbb{1} \rangle_{|0\rangle} = (-1)^{\alpha+\beta} \begin{vmatrix} G_1 & \cdots & G_{\alpha-1} & G_{\alpha+1} & \cdots & G_{\alpha+\beta} \\ \vdots & & \vdots & \vdots & & \vdots \\ G_{-\alpha+2} & \cdots & G_0 & G_2 & \cdots & G_{\beta+1} \\ G_{-\alpha} & \cdots & G_{-2} & G_0 & \cdots & G_{\beta-1} \\ \vdots & & \vdots & \vdots & & \vdots \\ G_{-\alpha-\beta+2} & \cdots & G_{-\beta} & G_{-\beta+2} & \cdots & G_1 \end{vmatrix}, \tag{A42}$$

$\langle \sigma_i^y \sigma_j^z \mathbb{1} \sigma_l^y \rangle_{|0\rangle} : \beta \to \beta + \delta$, $\langle \sigma_i^y \mathbb{1} \sigma_k^z \sigma_l^y \rangle_{|0\rangle} : \beta \to \delta \wedge \alpha \to \alpha + \beta$, and $\langle \mathbb{1} \sigma_j^y \sigma_k^z \sigma_l^y \rangle_{|0\rangle} : \beta \to \delta \wedge \alpha \to \beta$.

$$\langle \sigma_i^z \sigma_j^y \sigma_k^y \mathbb{1} \rangle_{|0\rangle} = (-1)^{\beta+1} \begin{vmatrix} G_0 & G_{\alpha+1} & \cdots & G_{\alpha+\beta} \\ G_{-\alpha} & G_1 & \cdots & G_\beta \\ \vdots & \vdots & & \vdots \\ G_{-\alpha-\beta+1} & G_{-\beta+2} & \cdots & G_1 \end{vmatrix}, \tag{A43}$$

$\langle \sigma_i^z \sigma_j^y \mathbb{1} \sigma_l^y \rangle_{|0\rangle} : \beta \to \beta + \delta$, $\langle \sigma_i^z \mathbb{1} \sigma_k^y \sigma_l^y \rangle_{|0\rangle} : \beta \to \delta \wedge \alpha \to \alpha + \beta$, and $\langle \mathbb{1} \sigma_j^z \sigma_k^y \sigma_l^y \rangle_{|0\rangle} : \beta \to \delta \wedge \alpha \to \beta$.

$$\langle \sigma_i^x \sigma_j^x \sigma_k^z \sigma_l^z \rangle_{|0\rangle} = (-1)^\alpha \begin{vmatrix} G_{-1} & \cdots & G_{\alpha-2} & G_{\alpha+\beta-1} & G_{\alpha+\beta+\delta-1} \\ \vdots & & \vdots & \vdots & \vdots \\ G_{-\alpha} & \cdots & G_{-1} & G_\beta & G_{\beta+\delta} \\ G_{-\alpha-\beta} & \cdots & G_{-\beta-1} & G_0 & G_\delta \\ G_{-\alpha-\beta-\delta} & \cdots & G_{-\beta-\delta-1} & G_{-\delta} & G_0 \end{vmatrix}, \tag{A44}$$

$$\langle \sigma_i^z \sigma_j^z \sigma_k^x \sigma_l^x \rangle_{|0\rangle} = (-1)^\delta \begin{vmatrix} G_0 & G_\alpha & G_{\alpha+\beta} & \cdots & G_{\alpha+\beta+\delta-1} \\ G_{-\alpha} & G_0 & G_\beta & \cdots & G_{\beta+\delta-1} \\ G_{-\alpha-\beta-1} & G_{-\beta-1} & G_{-1} & \cdots & G_{\delta-2} \\ \vdots & \vdots & \vdots & & \vdots \\ G_{-\alpha-\beta-\delta} & G_{-\beta-\delta} & G_{-\delta} & \cdots & G_{-1} \end{vmatrix}, \tag{A45}$$

$$\langle \sigma_i^z \sigma_j^x \sigma_k^x \sigma_l^z \rangle_{|0\rangle} = (-1)^\beta \begin{vmatrix} G_0 & G_\alpha & \cdots & G_{\alpha+\beta-1} & G_{\alpha+\beta+\delta} \\ G_{-\alpha-1} & G_{-1} & \cdots & G_{\beta-2} & G_{\beta+\delta-1} \\ \vdots & \vdots & & \vdots & \vdots \\ G_{-\alpha-\beta} & G_{-\beta} & \cdots & G_{-1} & G_\delta \\ G_{-\alpha-\beta-\delta} & G_{-\beta-\delta} & \cdots & G_{-\delta-1} & G_0 \end{vmatrix}, \quad (A46)$$

$$\langle \sigma_i^x \sigma_j^z \sigma_k^z \sigma_l^x \rangle_{|0\rangle} = (-1)^{\alpha+\beta+\delta} \begin{vmatrix} G_{-1} & \cdots & G_{\alpha-2} & G_\alpha & \cdots & G_{\alpha+\beta-2} & G_{\alpha+\beta} & \cdots & G_{\alpha+\beta+\delta-2} \\ \vdots & & \vdots & \vdots & & \vdots & \vdots & & \vdots \\ G_{-\alpha+1} & \cdots & G_0 & G_2 & \cdots & G_\beta & G_{\beta+2} & \cdots & G_{\beta+\delta} \\ G_{-\alpha-1} & \cdots & G_{-2} & G_0 & \cdots & G_{\beta-2} & G_\beta & \cdots & G_{\beta+\delta-2} \\ \vdots & & \vdots & \vdots & & \vdots & \vdots & & \vdots \\ G_{-\alpha-\beta+1} & \cdots & G_{-\beta} & G_{-\beta+2} & \cdots & G_0 & G_2 & \cdots & G_\delta \\ G_{-\alpha-\beta-1} & \cdots & G_{-\beta-2} & G_{-\beta} & \cdots & G_{-2} & G_0 & \cdots & G_{\delta-2} \\ \vdots & & \vdots & \vdots & & \vdots & \vdots & & \vdots \\ G_{-\alpha-\beta-\delta} & \cdots & G_{-\beta-\delta-1} & G_{-\beta-\delta+1} & \cdots & G_{-\delta-1} & G_{-\delta+1} & \cdots & G_{-1} \end{vmatrix}, \quad (A47)$$

$$\langle \sigma_i^y \sigma_j^y \sigma_k^z \sigma_l^z \rangle_{|0\rangle} = (-1)^\alpha \begin{vmatrix} G_1 & \cdots & G_\alpha & G_{\alpha+\beta} & G_{\alpha+\beta+\delta} \\ \vdots & & \vdots & \vdots & \vdots \\ G_{-\alpha+2} & \cdots & G_1 & G_{\beta+1} & G_{\beta+\delta+1} \\ G_{-\alpha-\beta+1} & \cdots & G_{-\beta} & G_0 & G_\delta \\ G_{-\alpha-\beta-\delta+1} & \cdots & G_{-\beta-\delta} & G_{-\delta} & G_0 \end{vmatrix}, \quad (A48)$$

$$\langle \sigma_i^z \sigma_j^z \sigma_k^y \sigma_l^y \rangle_{|0\rangle} = (-1)^\delta \begin{vmatrix} G_0 & G_\alpha & G_{\alpha+\beta+1} & \cdots & G_{\alpha+\beta+\delta} \\ G_{-\alpha} & G_0 & G_{\beta+1} & \cdots & G_{\beta+\delta} \\ G_{-\alpha-\beta} & G_{-\beta} & G_1 & \cdots & G_\delta \\ \vdots & \vdots & \vdots & & \vdots \\ G_{-\alpha-\beta-\delta+1} & G_{-\beta-\delta+1} & G_{-\delta+2} & \cdots & G_1 \end{vmatrix}, \quad (A49)$$

$$\langle \sigma_i^z \sigma_j^y \sigma_k^y \sigma_l^z \rangle_{|0\rangle} = (-1)^\beta \begin{vmatrix} G_0 & G_{\alpha+1} & \cdots & G_{\alpha+\beta} & G_{\alpha+\beta+\delta} \\ G_{-\alpha} & G_1 & \cdots & G_\beta & G_{\beta+\delta} \\ \vdots & \vdots & & \vdots & \vdots \\ G_{-\alpha-\beta+1} & G_{-\beta+2} & \cdots & G_1 & G_{\delta+1} \\ G_{-\alpha-\beta-\delta} & G_{-\beta-\delta+1} & \cdots & G_{-\delta} & G_0 \end{vmatrix}, \quad (A50)$$

$$\langle \sigma_i^y \sigma_j^z \sigma_k^z \sigma_l^y \rangle_{|0\rangle} = (-1)^{\alpha+\beta+\delta} \begin{vmatrix} G_1 & \cdots & G_{\alpha-1} & G_{\alpha+1} & \cdots & G_{\alpha+\beta-1} & G_{\alpha+\beta+1} & \cdots & G_{\alpha+\beta+\delta} \\ \vdots & & \vdots & \vdots & & \vdots & \vdots & & \vdots \\ G_{-\alpha+2} & \cdots & G_0 & G_2 & \cdots & G_\beta & G_{\beta+2} & \cdots & G_{\beta+\delta+1} \\ G_{-\alpha} & \cdots & G_{-2} & G_0 & \cdots & G_{\beta-2} & G_\beta & \cdots & G_{\beta+\delta-1} \\ \vdots & & \vdots & \vdots & & \vdots & \vdots & & \vdots \\ G_{-\alpha-\beta+2} & \cdots & G_{-\beta} & G_{-\beta+2} & \cdots & G_0 & G_2 & \cdots & G_{\delta+1} \\ G_{-\alpha-\beta} & \cdots & G_{-\beta-2} & G_{-\beta} & \cdots & G_{-2} & G_0 & \cdots & G_{\delta-1} \\ \vdots & & \vdots & \vdots & & \vdots & \vdots & & \vdots \\ G_{-\alpha-\beta-\delta+2} & \cdots & G_{-\beta-\delta} & G_{-\beta-\delta+2} & \cdots & G_{-\delta} & G_{-\delta+2} & \cdots & G_1 \end{vmatrix}, \quad (A51)$$

$$\langle \sigma_i^x \sigma_j^z \sigma_k^x \sigma_l^z \rangle_{|0\rangle} = (-1)^{\alpha+\beta+1} \begin{vmatrix} G_{-1} & \cdots & G_{\alpha-2} & G_{\alpha} & \cdots & G_{\alpha+\beta-2} & G_{\alpha+\beta+\delta-1} \\ \vdots & & \vdots & \vdots & & \vdots & \vdots \\ G_{-\alpha+1} & \cdots & G_0 & G_2 & \cdots & G_{\beta} & G_{\beta+\delta+1} \\ G_{-\alpha-1} & \cdots & G_{-2} & G_0 & \cdots & G_{\beta-2} & G_{\beta+\delta-1} \\ \vdots & & \vdots & \vdots & & \vdots & \vdots \\ G_{-\alpha-\beta} & \cdots & G_{-\beta-1} & G_{-\beta+1} & \cdots & G_{-1} & G_{\delta} \\ G_{-\alpha-\beta-\delta} & \cdots & G_{-\beta-\delta-1} & G_{-\beta-\delta+1} & \cdots & G_{-\delta-1} & G_0 \end{vmatrix}, \tag{A52}$$

$$\langle \sigma_i^z \sigma_j^x \sigma_k^z \sigma_l^x \rangle_{|0\rangle} = (-1)^{\beta+\delta+1} \begin{vmatrix} G_0 & G_{\alpha} & \cdots & G_{\alpha+\beta-1} & G_{\alpha+\beta+1} & \cdots & G_{\alpha+\beta+\delta-1} \\ G_{-\alpha-1} & G_{-1} & \cdots & G_{\beta-2} & G_{\beta} & \cdots & G_{\beta+\delta-2} \\ \vdots & \vdots & & \vdots & \vdots & & \vdots \\ G_{-\alpha-\beta+1} & G_{-\beta+1} & \cdots & G_0 & G_2 & \cdots & G_{\delta} \\ G_{-\alpha-\beta-1} & G_{-\beta-1} & \cdots & G_{-2} & G_0 & \cdots & G_{\delta-2} \\ \vdots & \vdots & & \vdots & \vdots & & \vdots \\ G_{-\alpha-\beta-\delta} & G_{-\beta-\delta} & \cdots & G_{-\delta-1} & G_{-\delta+1} & \cdots & G_{-1} \end{vmatrix}, \tag{A53}$$

$$\langle \sigma_i^y \sigma_j^z \sigma_k^y \sigma_l^z \rangle_{|0\rangle} = (-1)^{\alpha+\beta+1} \begin{vmatrix} G_1 & \cdots & G_{\alpha-1} & G_{\alpha+1} & \cdots & G_{\alpha+\beta} & G_{\alpha+\beta+\delta} \\ \vdots & & \vdots & \vdots & & \vdots & \vdots \\ G_{-\alpha+2} & \cdots & G_0 & G_2 & \cdots & G_{\beta+1} & G_{\beta+\delta+1} \\ G_{-\alpha} & \cdots & G_{-2} & G_0 & \cdots & G_{\beta-1} & G_{\beta+\delta-1} \\ \vdots & & \vdots & \vdots & & \vdots & \vdots \\ G_{-\alpha-\beta+2} & \cdots & G_{-\beta} & G_{-\beta+2} & \cdots & G_1 & G_{\delta+1} \\ G_{-\alpha-\beta-\delta+1} & \cdots & G_{-\beta-\delta-1} & G_{-\beta-\delta+1} & \cdots & G_{-\delta} & G_0 \end{vmatrix}, \tag{A54}$$

$$\langle \sigma_i^z \sigma_j^y \sigma_k^z \sigma_l^y \rangle_{|0\rangle} = (-1)^{\beta+\delta+1} \begin{vmatrix} G_0 & G_{\alpha+1} & \cdots & G_{\alpha+\beta-1} & G_{\alpha+\beta+1} & \cdots & G_{\alpha+\beta+\delta} \\ G_{-\alpha} & G_1 & \cdots & G_{\beta-1} & G_{\beta+1} & \cdots & G_{\beta+\delta} \\ \vdots & \vdots & & \vdots & \vdots & & \vdots \\ G_{-\alpha-\beta+1} & G_{-\beta+2} & \cdots & G_0 & G_2 & \cdots & G_{\delta+1} \\ G_{-\alpha-\beta-1} & G_{-\beta} & \cdots & G_{-2} & G_0 & \cdots & G_{\delta-1} \\ \vdots & \vdots & & \vdots & \vdots & & \vdots \\ G_{-\alpha-\beta-\delta+1} & G_{-\beta-\delta-2} & \cdots & G_{-\delta} & G_{-\delta+2} & \cdots & G_1 \end{vmatrix}, \tag{A55}$$

$$\langle \sigma_i^x \sigma_j^x \sigma_k^y \sigma_l^y \rangle_{|0\rangle} = (-1)^{\alpha+\delta} \begin{vmatrix} G_{-1} & \cdots & G_{\alpha-2} & G_{\alpha+\beta} & \cdots & G_{\alpha+\beta+\delta-1} \\ \vdots & & \vdots & \vdots & & \vdots \\ G_{-\alpha} & \cdots & G_{-1} & G_{\beta+1} & \cdots & G_{\beta+\delta} \\ G_{-\alpha-\beta} & \cdots & G_{-\beta-1} & G_1 & \cdots & G_{\delta} \\ \vdots & & \vdots & \vdots & & \vdots \\ G_{-\alpha-\beta-\delta+1} & \cdots & G_{-\beta-\delta} & G_{-\delta+2} & \cdots & G_1 \end{vmatrix}, \tag{A56}$$

$$\langle \sigma_i^y \sigma_j^y \sigma_k^x \sigma_l^x \rangle_{|0\rangle} = (-1)^{\alpha+\delta} \begin{vmatrix} G_1 & \cdots & G_{\alpha} & G_{\alpha+\beta} & \cdots & G_{\alpha+\beta+\delta-1} \\ \vdots & & \vdots & \vdots & & \vdots \\ G_{-\alpha+2} & \cdots & G_1 & G_{\beta+1} & \cdots & G_{\beta+\delta} \\ G_{-\alpha-\beta} & \cdots & G_{-\beta-1} & G_{-1} & \cdots & G_{\delta-2} \\ \vdots & & \vdots & \vdots & & \vdots \\ G_{-\alpha-\beta-\delta+1} & \cdots & G_{-\beta-\delta} & G_{-\delta} & \cdots & G_{-1} \end{vmatrix}, \tag{A57}$$

$$\langle \sigma_i^x \sigma_j^y \sigma_k^y \sigma_l^x \rangle_{|0\rangle} = (-1)^{\alpha+\delta} \begin{vmatrix} G_{-1} & \cdots & G_{\alpha-1} & G_{\alpha+\beta} & \cdots & G_{\alpha+\beta+\delta-2} \\ \vdots & & \vdots & \vdots & & \vdots \\ G_{-\alpha+1} & \cdots & G_1 & G_{\beta+2} & \cdots & G_{\beta+\delta} \\ G_{-\alpha-\beta} & \cdots & G_{-\beta} & G_1 & \cdots & G_{\delta-1} \\ \vdots & & \vdots & \vdots & & \vdots \\ G_{-\alpha-\beta-\delta} & \cdots & G_{-\beta-\delta} & G_{-\delta+1} & \cdots & G_{-1} \end{vmatrix}, \tag{A58}$$

$$\langle \sigma_i^y \sigma_j^x \sigma_k^x \sigma_l^y \rangle_{|0\rangle} = (-1)^{\alpha+\delta} \begin{vmatrix} G_{1} & \cdots & G_{\alpha-1} & G_{\alpha+\beta} & \cdots & G_{\alpha+\beta+\delta} \\ \vdots & & \vdots & \vdots & & \vdots \\ G_{-\alpha+1} & \cdots & G_{-1} & G_{\beta} & \cdots & G_{\beta+\delta} \\ G_{-\alpha-\beta} & \cdots & G_{-\beta-2} & G_{-1} & \cdots & G_{\delta-1} \\ \vdots & & \vdots & \vdots & & \vdots \\ G_{-\alpha-\beta-\delta+2} & \cdots & G_{-\beta-\delta} & G_{-\delta+1} & \cdots & G_{1} \end{vmatrix}, \tag{A59}$$

$$\langle \sigma_i^x \sigma_j^x \sigma_k^x \sigma_l^x \rangle_{|0\rangle} = (-1)^{\alpha+\delta} \begin{vmatrix} G_{-1} & \cdots & G_{\alpha-2} & G \cdots & G_{\alpha+\beta+\delta-2} \\ \vdots & & \vdots & \vdots & & \vdots \\ G_{-\alpha} & \cdots & G_{-1} & G_{\beta} & \cdots & G_{\beta+\delta-1} \\ G_{-\alpha-\beta-1} & \cdots & G_{-\beta-2} & G_{-1} & \cdots & G_{\delta-2} \\ \vdots & & \vdots & \vdots & & \vdots \\ G_{-\alpha-\beta-\delta} & \cdots & G_{-\beta-\delta-1} & G_{-\delta} & \cdots & G_{-1} \end{vmatrix}, \tag{A60}$$

$$\langle \sigma_i^y \sigma_j^y \sigma_k^y \sigma_l^y \rangle_{|0\rangle} = (-1)^{\alpha+\delta} \begin{vmatrix} G_{1} & \cdots & G_{\alpha} & G_{\alpha+\beta+1} & \cdots & G_{\alpha+\beta+\delta} \\ \vdots & & \vdots & \vdots & & \vdots \\ G_{-\alpha+2} & \cdots & G_{1} & G_{\beta+2} & \cdots & G_{\beta+\delta+1} \\ G_{-\alpha-\beta+1} & \cdots & G_{-\beta} & G_{1} & \cdots & G_{\delta} \\ \vdots & & \vdots & \vdots & & \vdots \\ G_{-\alpha-\beta-\delta+2} & \cdots & G_{-\beta-\delta+1} & G_{-\delta+2} & \cdots & G_{1} \end{vmatrix}. \tag{A61}$$

[1] A. Osterloh, L. Amico, G. Falci, and R. Fazio, Nature (London) **416**, 608 (2002).

[2] T. J. Osborne and M. A. Nielsen, Phys. Rev. A **66**, 032110 (2002).

[3] G. Vidal, J. I. Latorre, E. Rico, and A. Kitaev, Phys. Rev. Lett. **90**, 227902 (2003).

[4] L. A. Wu, M. S. Sarandy, and D. A. Lidar, Phys. Rev. Lett. **93**, 250404 (2004).

[5] T. Roscilde, P. Verrucchi, A. Fubini, S. Haas, and V. Tognetti, Phys. Rev. Lett. **93**, 167203 (2004).

[6] For recent results, see P. Nataf, M. Dogan, and K. Le Hur, Phys. Rev. A **86**, 043807 (2012); Y. Yao, H.-W. Li, Ch.-M. Zhang, Zh.-Q. Yin, W. Chen, G.-C. Guo, and Zh.-F. Han, *ibid.* **86**, 042102 (2012); F. Altintas and R. Eryigit, Ann. Phys. (NY) **327**, 3084 (2012); L. Lepori, G. De Chiara, and A. Sanpera, Phys. Rev. B **87**, 235107 (2013); V. Azimi Mousolou, C. M. Canali, and E. Sjöqvist, Phys. Rev. A **88**, 012310 (2013); for a review, see L. Amico, R. Fazio, A. Osterloh, and V. Vedral, Rev. Mod. Phys. **80**, 517 (2008).

[7] For reviews, see F. Verstraete, J. I. Cirac, and V. Murg, Adv. Phys. **57**, 143 (2008); N. Schuch, arXiv:1306.5551.

[8] D. Patanè, R. Fazio, and L. Amico, New J. Phys. **9**, 322 (2007).

[9] S. M. Giampaolo and B. C. Hiesmayr, Phys. Rev. A **88**, 052305 (2013).

[10] J. Stasińska, B. Rogers, M. Paternostro, G. De Chiara, and A. Sanpera, Phys. Rev. A **89**, 032330 (2014).

[11] T.-C. Wei, D. Das, S. Mukhopadyay, S. Vishveshwara, and P. M. Goldbart, Phys. Rev. A **71**, 060305(R) (2005); O. Gühne, G. Tóth, and H. J. Briegel, New J. Phys. **7**, 229 (2005); R. Orús, Phys. Rev. Lett. **100**, 130502 (2008); H. S. Dhar, A. Sen(De), and U. Sen, *ibid.* **111**, 070501 (2013); New J. Phys. **15**, 013043 (2013).

[12] M. Srednicki, Phys. Rev. Lett. **71**, 666 (1993); C. Holzhey, F. Larsen, and F. Wilczek, Nucl. Phys. B **424**, 443 (1994); V. E. Korepin, Phys. Rev. Lett. **92**, 096402 (2004); M. B. Hastings, J. Stat. Mech. (2007) P08024; G. Vitagliano, A. Riera, and J. I. Latorre, New J. Phys. **12**, 113049 (2010); P. Calabrese, M. Mintchev, and E. Vicari, Eur. Phys. Lett. **97**, 20009 (2012);

P. Zanardi and L. C. Venuti, J. Stat. Mech. (2013) P04023; J. Haegeman, T. J. Osborne, H. Verschelde, and F. Verstraete, Phys. Rev. Lett. **110**, 100402 (2013); B. Collins, I. Nechita, and K. Zyczkowski, J. Phys. A: Math. Theor. **46**, 305302 (2013).

[13] J. Eisert, M. Cramer, and M. B. Plenio, Rev. Mod. Phys. **82**, 277 (2010).

[14] J. Batle and M. Casas, Phys. Rev. A **82**, 062101 (2010).

[15] B. Jungnitsch, T. Moroder, and O. Gühne, Phys. Rev. Lett. **106**, 190502 (2011).

[16] J. T. Barreiro, P. Schindler, O. Gühne, T. Monz, M. Chwalla, C. F. Roos, M. Hennrich, and R. Blatt, Nat. Phys. **6**, 943 (2010); H. Kampermann, O. Gühne, C. Wilmott, and D. Bruß, Phys. Rev. A **86**, 032307 (2012).

[17] E. Lieb, T. Schultz, and D. Mattis, Ann. Phys. (NY) **16**, 407 (1961); P. Pfeuty, ibid. **57**, 79 (1970); E. Barouch, B. M. McCoy, and M. Dresden, Phys. Rev. A **2**, 1075 (1970); E. Barouch, B. M. McCoy, and M. Barry, ibid. **3**, 786 (1971).

[18] Sometimes the notion of "genuine multiparticle entanglement" is used in a more strict way, by requiring in addition that the state has a nonvanishing value of some globally SL-invariant quantity [32]. These states are discerned by states in the null cone of global SL invariance.

[19] O. Gühne and G. Tóth, Phys. Rep. **474**, 1 (2009).

[20] Formally, the partial transposition of a bipartite state $\varrho = \sum_{ij,kl} \varrho_{ij,kl} |i\rangle\langle j| \otimes |k\rangle\langle l|$ with respect to the second system is defined as $\varrho^{T_B} = \sum_{ij,kl} \varrho_{ij,kl} |i\rangle\langle j| \otimes |l\rangle\langle k|$.

[21] A. Peres, Phys. Rev. Lett. **77**, 1413 (1996).

[22] O. Gühne, B. Jungnitsch, T. Moroder, and Y. S. Weinstein, Phys. Rev. A **84**, 052319 (2011); L. Novo, T. Moroder, and O. Gühne, ibid. **88**, 012305 (2013).

[23] M. E. Fisher, in Fenomeni Critici, edited by M. S. Green (Academic, New York, 1971).

[24] M. N. Barber, in Phase Transitions and Critical Phenomena, edited by C. Domb and J. L. Lebowitz (Academic, New York, 1983).

[25] In many systems the shift exponent κ equals the inverse of critical exponent ν of the diverging correlation length [24]. In our case, however, this turns out not to be the case.

[26] But note that the argument of Ref. [4] in the strict sense concerns only entanglement in k-particle marginals of a ground state of a k-body Hamiltonian.

[27] A. Uhlmann, Phys. Rev. A **62**, 032307 (2000).

[28] A. Sen(De), U. Sen, and M. Lewenstein, Phys. Rev. A **72**, 052319 (2005).

[29] See the program PPTMIXER, available at mathworks.com/matlabcentral/fileexchange/30968.

[30] L. Gurvits and H. Barnum, Phys. Rev. A **66**, 062311 (2002).

[31] E. R. Caianiello and S. Fubini, Nuovo Cimento **9**, 1218 (1952).

[32] A. Osterloh and J. Siewert, Phys. Rev. A **72**, 012337 (2005).